Acta Polytechnica **63**(6):411–418, 2023
https://doi.org/10.14311/AP.2023.63.0411

Published by the Czech Technical University in Prague

MONITORING THE INTERNAL STRUCTURE BEHAVIOUR OF ALKALI-ACTIVATED SLAG PASTE: EFFECT OF THE CURING MODE

Petr Nápravník[a,*], Dalibor Kocáb[a], Vlastimil Bílek, Jr.[b], Dominik Lisztwan[a], Barbara Kucharczyková[a]

[a] *Brno University of Technology, Faculty of Civil Engineering, Institute of Building Testing, Veveří 331/95, 602 00 Brno, Czech Republic*

[b] *Brno University of Technology, Faculty of Chemistry, Institute of Materials Science, Purkyňova 464/118, 612 00 Brno, Czech Republic*

[*] corresponding author: Petr.Napravnik1@vutbr.cz

Abstract. This paper deals with the monitoring of the internal structure behaviour of an alkali-activated slag (AAS) paste. The slag was activated with a 4M solution of sodium hydroxide. The behaviour of the internal structure of the paste was regularly monitored through the changes in the resonant frequency and the mechanical properties, until the paste reached the age of 90 days. The main aim of the article is to show the long-term maturation and degradation process of an AAS paste under different curing modes. The results obtained suggest that the curing mode of the specimens has a significant effect on the behaviour of the internal structure of the paste based on the AAS. The development of both the dynamic properties and the flexural strength indicates the occurrence of a higher porosity in the internal structure of the paste, especially when the free drying process is started earlier. Insufficient hydration of the binder system is also a likely cause of cracks. The reduction in the relative dynamic moduli values ranging from 50 % to 80 % was observed for drying specimens at the age of 90 days. What is very interesting is that the occurrence of cracks was not prevented even by intensive moist curing of the paste as, between the 21st and the 28th day of maturing, there was a significant decrease of about 20 % in the relative dynamic modulus of elasticity and also a 50 % reduction in the flexural strength.

Keywords: Alkali-activated slag, resonance method, resonant frequency, curing mode, flexural strength, crack.

1. Introduction

The relatively high CO_2 emissions associated with the production of Portland cement are leading to increasing interest in alternative inorganic binders, including alkali-activated slag (AAS). These are binders in which the reaction of the ground granulated blast furnace slag is supported by the presence of an activator with high alkalinity. Apart from the environmental aspect, the main advantages of AAS materials include the resistance to an aggressive environment [1–3], resistance to high temperatures [4], and a fast increase in strength [5]. However, the main drawback is undoubtedly the tendency for significant shrinkage, accompanied by the occurrence of cracks, which limits the wider use of AAS materials in practice. One must realise that the resulting properties of these materials greatly depend on the type of the activator used, its concentration, the ratio of the precursor to the activation solution, or the curing conditions. The commonly used alkaline activators include hydroxides, silicates, and other alkali metal salts, most commonly sodium. The type of activator itself significantly affects the hydration process in AAS materials, which crucially influences their resulting physical and mechanical properties. For example, with water glass activation, high ultimate compressive strengths and good workability can be reached [6]. However, there is a risk of massive autogenous shrinkage [7, 8] and shrinkage due to drying, which is usually accompanied by the occurrence of cracks. On the contrary, AAS based on the sodium hydroxide activator has a significant increase in the initial compressive strength, due to a high hydration rate. However, the further increase in the compressive strength is not as significant as for the other activators. One of the main reasons given is a slow decrease in capillary porosity [6, 9, 10].

The current state of the microstructure, in terms of pore size and distribution or the extent of damage caused by cracks can be described using microscopic methods or mercury porosimetry [11]. However, both of these methods are destructive and require careful sample preparation, which are often obtained from larger specimens. A sample obtained in this way is significantly smaller than the size of the original specimen and, therefore, it is not possible to fully describe the distribution of pores or the extent of material damage throughout the entire volume. More suitable approach for this particular purpose is the use of non-

destructive methods (NDT), which are sensitive to the presence of local defects and cracks. This field includes a wide range of methods, for example, the ultrasonic pulse velocity method, or resonance method, which were also used in the experiment herein. The extent of damage to the internal structure can be monitored through a decrease in the dynamic modulus of elasticity. In principle, the assessment can be the same as when testing the freeze-thaw resistance of concrete according to ASTM C666/C666M-15 [12] or CEN/TR 15177 [13]. In these cases, a change in the dynamic modulus of elasticity is presented through the relative dynamic modulus of elasticity (RDM). It can be determined by either of the above NDT methods. However, the resonance method turned out to be much more suitable for this purpose as it reacts considerably more sensitively to the internal structure defects – it shows a considerably higher decrease in the dynamic modulus of elasticity than the ultrasonic pulse method [14]. An advantage of the resonance method is not only its non-destructive character, which makes it possible to perform the measurement repeatedly on the same specimen over indefinitely, reducing the number of specimens required, but also the ability to calculate of more dynamic properties of the material at once. Besides the dynamic Young's modulus, which can be calculated based on the natural frequency of both the longitudinal and transverse vibrations, the dynamic shear modulus of elasticity and the dynamic Poisson's ratio can also be determined. This enables a better description of the behaviour of the material's internal structure both in terms of its maturation and in terms of the damage caused by degradation mechanisms.

The article presents a novel approach to the long-term assessment of the maturation of alkali-activated materials, which are susceptible to internal structure damage without visual surface defects. The presented non-destructive method provides long-term data without the variability of different test sets typical of destructive testing. In addition, the method appears to be promising as an effective monitoring tool in the design of new compositions of AAS materials.

2. Experiment details

Three groups of test specimens from alkali-activated slag differing only in the curing regime were prepared for this experiment. The slag was activated with sodium hydroxide. The main parameters monitored were the resonant frequencies, and the flexural and compressive strength, depending on the age of the test sets and the curing mode method used during their maturation.

Before demoulding, all the specimens were left to mature at a standard laboratory temperature of $20 \pm 2\,^{\circ}\mathrm{C}$ and normal atmospheric pressure for the first 24 hours after casting. The top surface of the specimens in the moulds was covered with a PE film to prevent them from drying. After demoulding, the specimens were divided into three sets, for which three different curing modes were selected. The first group was allowed to dry freely immediately after demoulding in an air-conditioned laboratory at a temperature of $22 \pm 2\,^{\circ}\mathrm{C}$ and a relative humidity (RH) of $55 \pm 5\,\%$. The second group was stored after demolding in a chamber with a relative humidity of $\geq 95\,\%$ and, after 28 days, was allowed to dry freely under the same conditions as the first set. The third group, designated as the reference one, was stored in a chamber with a relative humidity of $\geq 95\,\%$ for the entire measuring period. The development of the resonant frequencies over time was monitored in all of the test sets. In the reference set, the flexural strength and the compressive strength were also determined at selected ages. The paper presents the results for AAS pastes of the age of up to 90 days.

2.1. Material

As the aluminosilicate precursor needed for the preparation of the alkali-activated paste, ground granulated blast furnace slag (LB Cemix, s.r.o.) was used with a specific surface area by Blaine of $400\,\mathrm{m^2\,kg^{-1}}$ and the amorphous phase as the majority content. The slag was activated with a 4M solution of sodium hydroxide, which was prepared by diluting the initial 50 % solution of NaOH (Carl Roth GmbH + Co. KG) with demineralised water at least 24 hours in advance. The volume fraction of the slag in the paste was 0.52. This way of expressing the paste composition is based on the previous study [15], in which the aforementioned molarity seems to be close to the optimum in terms of the amount of heat developed during the hydration. The slag volume fraction was adjusted to achieve the desired consistency of the paste. Note that the mass ratio 4M NaOH solution to slag was 0.37.

The paste was prepared using the Hobart mixer. The total mixing time was 3 minutes; during the first 50 seconds, the slag was poured into the activator, weighed in advance. Immediately after the mixing of the paste was finished, its consistency was determined using a flow table test by EN 1015-3 [16] as well as its density by EN 1015-6 [17]. The diameter of the poured-out paste just after lifting the cone was 105 mm. After performing fifteen jolts, it spread to 164 mm. The density of the fresh paste was determined to be $2020\,\mathrm{kg\,m^{-3}}$. The fresh paste was used to fill in steel triple moulds with the nominal size of each part being $40\,\mathrm{mm} \times 40\,\mathrm{mm} \times 160\,\mathrm{mm}$. The molds were filled in two layers, and each of them was compacted using a high-frequency vibration table. For the purposes of the experiment, three test sets (for the measurement of resonant frequencies and mass losses) and nine additional test sets (for strength tests) were made, each set containing three specimens. The curing regime used for each test set after demoulding is introduced in Table 1.

The average density of the H_Ref, H_24h and H_28d sets were 2 000, 1 830 and $1\,930\,\mathrm{kg\,m^{-3}}$, respectively, at the age of 90 days.

Designation	Curing mode
H_Ref	stored constantly at RH $\geq$ 95 % (except for the testing periods)
H_24h	free drying in the air
H_28d	28 days at RH $\geq$ 95 %, then free drying in the air
H_1, H_3, H_7, H_14, H_25, H_28, H_35, H_56, H_91	stored at v RH $\geq$ 95 % until the time of testing

TABLE 1. Curing mode of each set of specimens after demoulding.

2.2. Measuring Methods

2.2.1. Determining the Natural Frequencies of the Specimens

The natural frequencies of vibration were measured at regular intervals for the specimens in the H_Ref, H_24h and H_28d sets. The first measurement for the reference set (H_Ref) was taken immediately after demoulding. Afterwards, the specimens were stored in a chamber with a relative humidity of $\geq$ 95 %. Shortly before each subsequent measurement, the specimens were taken out, surface dried, and their masses and natural frequencies of vibration were determined. Then, they were immediately returned to the chamber. In an analogous manner, the measurement was also performed on the second set (H_24h), the difference being that after the first measurement, the specimens were left to dry freely until the end of the measurement. The third set (H_28d) was stored immediately after demoulding in a chamber with a relative humidity of $\geq$ 95 % and the first measurement was performed at the age of 28 days, when they were first taken out of the chamber. For the remaining period, the specimens were left to dry freely. The free drying took place in an air-conditioned laboratory with a temperature of 22 $\pm$ 2 °C and a relative humidity of 55 $\pm$ 5 %. For each specimen of each set, the first natural frequencies of longitudinal vibration f_L, transverse vibration f_f, and torsional vibration f_t were determined as well as the mass for monitoring the mass losses. The measurement was performed at regular intervals over a period of 90 days. The natural frequencies were measured using an impulse hammer (exciter), acceleration sensor and oscilloscope. The evaluation software works on the principle of fast Fourier transform (see Figure 1). The measurements of the natural frequencies of the specimens and the determination of the dynamic Poisson's ratio were performed in accordance with ASTM C215-19 standard [18]. The frequencies measured were also used to determine the relative change in the dynamic moduli of elasticity (RDM) based on the procedure recommended by the standard [12]. The reference values considered for the calculation of RDM were the values of the dynamic moduli of elasticity of the H_Ref set determined in the first measurement performed at the age of 24 hours. The calculation was based on the Equation 1:

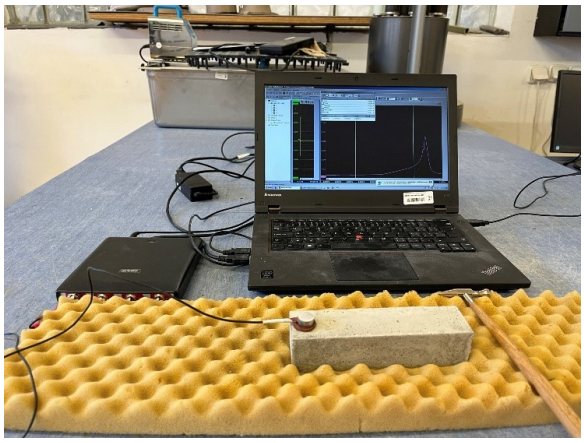

(A).

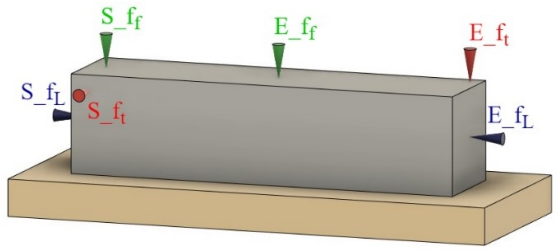

(B).

FIGURE 1. An illustrative picture showing the determination of the first natural frequency of transverse vibration (A), location of sensors (S_), and exciters (E_) for determining the first natural frequency of longitudinal f_L, transverse f_f, and torsional vibration f_t (B).

$$RDM_i\_f_L, f_t, f_f = \left(\frac{n_i^2}{n_1^2}\right) \cdot 100, \qquad (1)$$

where $RDM_i\_f_L, f_t, f_f$ are the values of the relative modulus of elasticity determined for the i$^{\text{th}}$ measurement, n_i are the values of f_L, f_t or f_f determined during the i$^{\text{th}}$ measurement, n_1 are the values of f_L, f_t or f_f determined during the first measurement performed on the test set H_Ref at the age of 24 hours.

2.2.2. Determining the strength parameters

To determine the strength parameters of the AAS pastes, a total of nine test sets were used, each containing three specimens with the nominal size of 40 mm × 40 mm × 160 mm (H_1, H_3, H_7, H_14, H_25, H_28, H_35, H_56, H_91). All specimens

were stored in a chamber with a relative humidity of $\geq 95\,\%$ until the time of testing. Before the test, they were taken out of the chamber, surface dried, and their mass and size were determined.

The flexural strength was determined according to EN 196-1 [19]. The specimens were subjected to the three-point bending test, in which the distance between the supports was set to 100 mm, and the force was placed in the middle of the span (see Figure 2b). The tests were performed on the LabTest 6.30 testing machine with a constant loading rate of $0.05\,\mathrm{MPa\,s^{-1}}$.

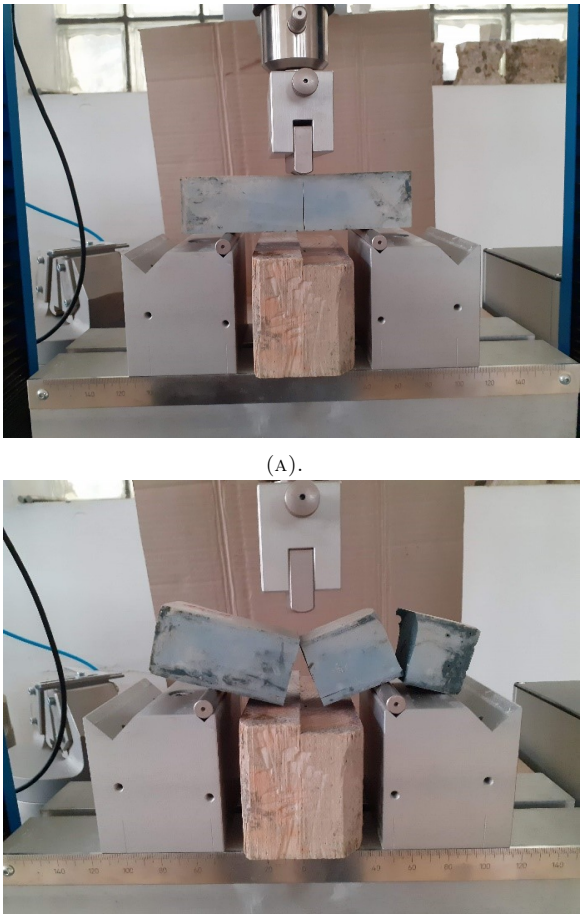

(A).

(B).

Figure 2. An example of failure modes of the specimens after the flexural strength test at the age of 28 days: correct (A), incorrect (B) failure mode of the specimen.

The compressive strength was determined using the specimen fractions that remained after the flexural strength test. The compressive strength was determined in accordance with the EN 196-1 standard [19]. The test was performed using the DELTA 6-300 hydraulic press (Form + Test Seidner & Co. GmbH) with a constant loading rate set to $0.6\,\mathrm{MPa\,s^{-1}}$. To mark the compression areas, a compressive strength test device was on the fractions with 40 mm × 40 mm hardened steel pressure plates with a thickness of 10 mm, which are part of the press.

3. Results

The results of the measurements are shown in the following figures as the mean of three independent measurements performed on the specimens from each test set. The compressive strength of the fractions is the mean value of six independent measurements. The variability of the results of the measurements, expressed through the sample standard deviation, is represented in the graphs using error bars.

Figure 3 shows the relative changes in the dynamic moduli of elasticity RDM_fL and RDM_ff. Figure 4 shows the relative changes in the dynamic modulus of elasticity RDM_ft and the development of the dynamic Poisson's ratio, which was calculated from the frequencies of the longitudinal and torsional vibrations.

In the reference set, a gradual increase can be seen in all three dynamic moduli of elasticity up to the age of approximately 21 days, which corresponds to the common trend for mechanical properties during the maturation of concrete materials at a high relative humidity [20–23]. The subsequent decrease in the modulus of elasticity indicates a change in the rigidity of the specimen, which may, in this case, suggest the occurrence of cracks or local defects in the structure of the material. The effect is similar to, for example, damage by cyclic freezing [24], or cycling loading in a fatigue test [25] where the resonance method was effectively used.

The recurring increase in RDM observed from the age of approximately 42 days may, on the contrary, indicate the closing of the cracks. A decrease in the dynamic modulus of elasticity is clearly apparent for RDM_fL and RDM_ff, while for RDM_ft the trend is not very strong.

In the set H_24h, which was left to dry freely for the entire measurement period, a slight increase in RDM_fL and RDM_ft can be observed at the beginning. However, from the age of 7 days, they begin to decrease gradually. RDM_ff has a decreasing tendency from the very beginning of the measurement. At the age of 90 days, the RDM_fL and RDM_ff values dropped to almost 20 % and RDM_ft to 40 %. The decreasing trend in the resonant frequencies and the RDM values calculated from them in the sets that were left to dry freely suggests a gradual increase in the porosity and occurrence of cracks in the structure of the material due to insufficient treatment [20]. A very similar trend can be observed in the set H_28d, whose modulus of elasticity was, at the time when the measurement started, the same as the modulus of elasticity of the reference set and decreased rapidly due to the subsequent exposure to free drying. At the time of the exposure to free drying, the degree of hydration of the binder system was much higher in the H_28d set than in the H_24h set, which may indicate a finer porosity of the internal structure in the H_28d set [9, 11]. Furthermore, it is necessary to realise that there were already cracks in the specimens when they

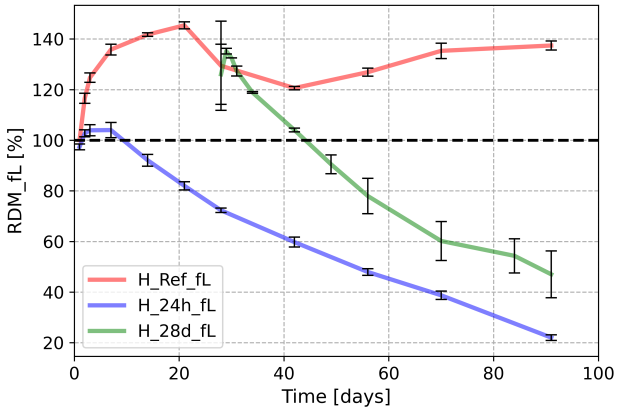

(A).

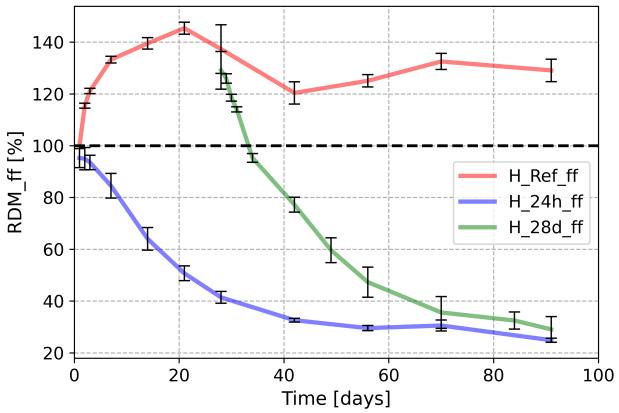

(B).

FIGURE 3. Relative change in the dynamic modulus of elasticity determined through longitudinal vibration (A) and transverse vibration (B).

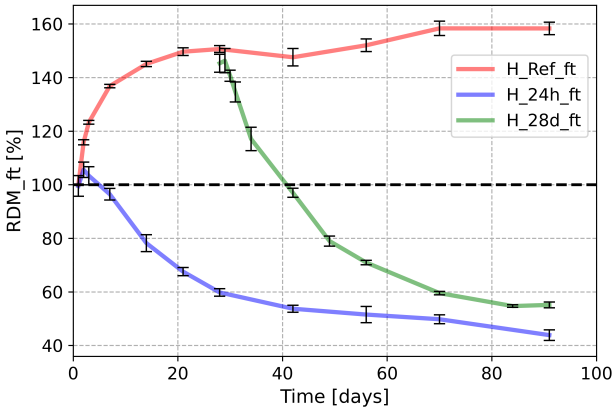

(A).

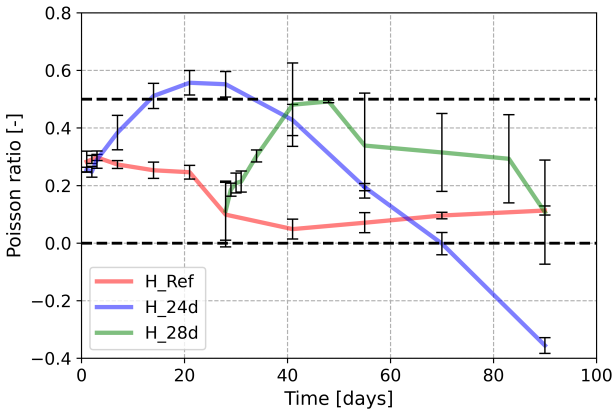

(B).

FIGURE 4. Relative change in the dynamic modulus of elasticity determined through torsional vibration (A) and the development of the dynamic Poisson's ratio (B).

were being taken out (see the development of RDM in the set H_Ref). The subsequent drying then led to an increase in the porosity and crack propagation. Moreover, due to the drying of the fine pores, additional internal stresses could have developed and, thus, new cracks could occur. At the age of 90 days, a decrease was observed in RDM_fL and RDM_ft to approximately 50 % and in RDM_ff as low as approximately 30 %.

Moreover, an uncommon evolution of the mean values of Poisson's ratio was observed for particular sets of specimens. The reference set shows the real development of Poisson's ratio up to the age of 21 days of maturation, which is approximately 0.25 over this period. Then, a decrease to 0 occurs, and from the age of 42 days, it starts growing again. This trend copies the development of RDM and indicates the propagation of cracks and their subsequent closing. Poisson's ratio of the H_24h set increases up to the age of 21 days and then drops rapidly. The highest value of Poisson's ratio was almost 0.6, and the lowest was almost −0.4. From the perspective of the behaviour of common solid substances, these values are not possible. They only demonstrate a disproportion between the natural frequencies of vibration of the specimens caused by the occurrence of defects and cracks in the internal structure of the material. The development of Poisson's ratio for the set H_28d is similar to that of the set H_24h – a gradual increase and, after 21 days of free drying, a decrease occurs. The increase and the decrease are less pronounced for the H_28d set and are accompanied by a high variability in the results.

The use of the resonance method for monitoring the development of the AAS paste quality has proven effective, primarily due to the non-destructive nature of the method used. The measurement intervals could be operatively adjusted according to the character of the investigated material to determine the cracking time. Employing destructive methods to determine the bending tensile strength would require a large number of test specimens, which would be highly inefficient. A slight disadvantage of the resonance method is that the exact reason for the crack occurrence cannot be assessed. This could be solved, for example, by using a computer tomography or scanning microscopy analysis. However, the usage of these methods would be labour and cost-intensive and require a special preparation of the specimens. Nevertheless, a suitable combination of the methods mentioned above should be a proper solution in future applications.

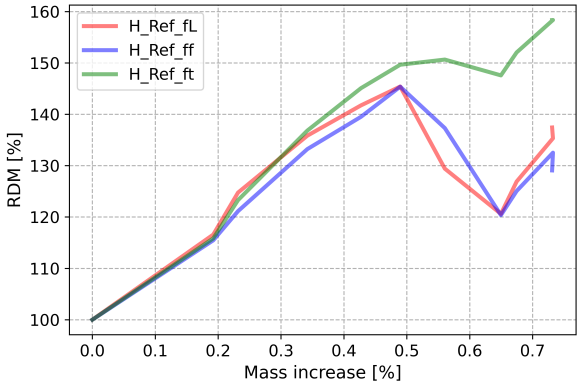

(A).

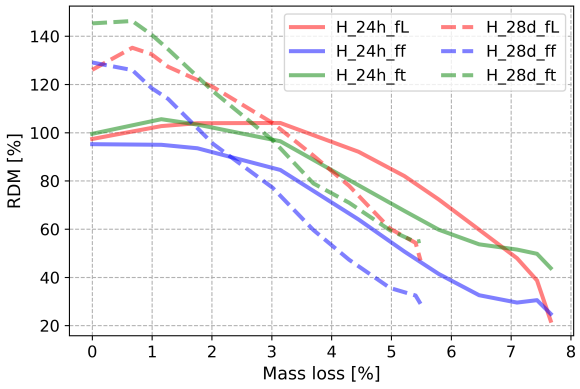

(B).

Figure 5. Dependence of RDM on the mass change of the reference set (A) and the H_24h and H_28d sets (B).

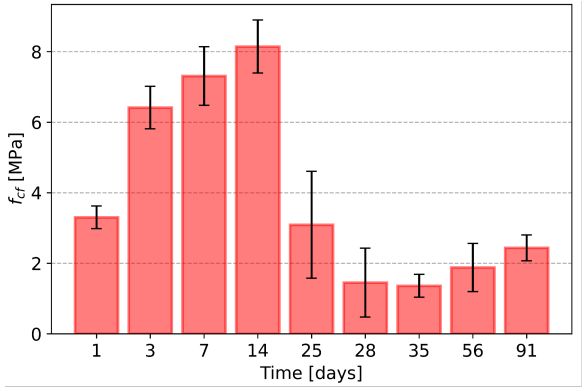

(A).

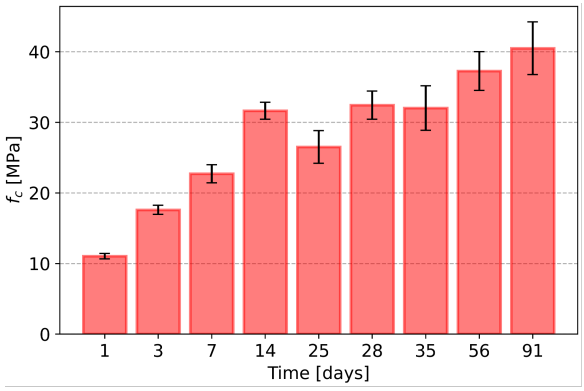

(B).

Figure 6. The strength characteristics of the test sets: the flexural strength f_{cf} (A), the compressive strength f_c (B)).

The drying process was monitored as an accompanying quantity. It is represented by the mass losses determined for each test set. On the contrary, in the reference set stored in an environment with RH $\geq$ 95 %, a mass increase was observed. The mass losses in the H_24h and H_28d sets follow a similar trend as the decrease in the resonant frequencies. However, they do not correspond completely with the extent of the decline in the RDM values. The dependence of RDM on the mass change of the specimens is shown in Figure 5. In the reference set, the mass of the specimens increased gradually, which led to a significant decrease in RDM between the 21$^{\text{st}}$ and the 42$^{\text{nd}}$ day of maturation, see Figure 5a. In Figure 5b, in can clearly be seen that the mass loss in the H_24h and H_28d sets is, to a certain extent, linearly dependent on RDM, especially for the H_28d set. The decline in the dynamic moduli of elasticity is partly caused by a loss of the material rigidity due to its porosity increasing as a result of drying. That alone, however, is not enough for the occurrence of such a significant decrease in RDM, as can be seen, for example, from the results published in [20, 23, 26]. Therefore, it can be assumed that during drying, microcracks are formed in the internal structure of the AAS paste.

Figure 6 shows the development of the flexural strength f_{cf} and the compressive strength f_c, which was determined on the fractions of the specimens after the flexural strength tests. The specimens were stored in the same environment as the H_Ref test set until the testing started. The average density for the specimens intended for the strength tests ranged from 1 970 to 1 990 kg m^{-3} within the time interval of the performed tests. The development of the flexural strength followed a similar trend to that of RDM_fL and RDM_ff for the reference set. Due to the formation and propagation of cracks, a significant decrease in flexural strength occurred between the 14$^{\text{th}}$ and 25$^{\text{th}}$ day of maturation. The relatively high variability of the results is probably related to the considerably uncontrolled formation and propagation of cracks. The network of cracks is obviously different in each sample, as can be seen in the illustrative picture of the damage in Figure 2b – correct failure in the middle of the span (on the left) and incorrect failure, when the specimen was broken up into several parts (on the right). From the compressive strength tests on the samples, it can be concluded that the presence of cracks does not cause a decrease in this value. However, from the age of 25 days, an increased variability of the results can be observed.

4. Conclusion

This paper presents the results of measurements performed on pastes made from slag activated by sodium hydroxide. The monitoring was mainly focused on the effect of the treatment of the specimens on the development of the physical and mechanical properties of the AAS paste. The specimens of the reference set were stored in an environment with RH $\geq$ 95 %for the entire maturation period. One of the two remaining sets was exposed to free drying from the age of 24 hours and the other from the age of 28 days. The behaviour of the internal structure was monitored non-destructively through the development of the dynamic characteristics of the material studied. The resonance method was used for this purpose. In order to monitor the development of the mechanical properties of the AAS paste, flexural and compressive strengths were determined for the specimens stored in an environment with RH $\geq$ 95 % at selected ages.

Based on the results obtained, the following conclusions can be made:

- The curing regime of the specimens has an important effect on the development of the resonant frequencies and, thus, significantly affects the development of the dynamic moduli of elasticity and Poissons ratio.
- For the test sets exposed to free drying (H_24h and H_28d), a decrease in the RDM_fL values was observed to 20 % (for H_24h) and 50 % (for H_28d) of the initial values measured for the reference set at the age of 24 hours immediately after demoulding. The RDM_ft showed the same final reduction for both sets at the age of 90 days. However, the slope of the decrease was steeper for the H_28d set. The results clearly show that the prolonged moist curing of the H_28d set did not prevent the steep decrease in the RDM values. The decrease in RDM for the H_24h set is mainly caused by the specimens drying very early, which led to the formation of increased porosity in the internal structure of the material and did not allow sufficient hydration of the binder system, which probably also led to the occurrence of cracks. For the specimens of the H_28d set, with a high degree of hydration and the related finer porosity, the drying could also lead to the development of additional internal stresses due to the fine pores drying and thus the formation of cracks (it is necessary to realise that the specimens of the H_28d set were already damaged with cracks when they were taken out into the air – see the RDM development for the H_Ref set). Both hypotheses are confirmed by the development of the Poisson's ratio values, which indicates that the internal structure of the specimens was significantly damaged by cracks in both the sets tested.
- In the reference set, despite intensive moist curing, a decrease in RDM was observed between the 21st and 28th day of maturation. At the same age, a decrease in the Poissons ratio values and in the flexural strength was also observed. This decrease again indicates the formation of cracks. A high variability of the results observed during this period points to an uneven and rather local occurrence of defects in the internal structure of the material. From the age of 42 days, an increase in RDM and flexural strength was observed again, indicating healing of the cracks due to the continued treatment at high relative humidity.
- The results presented in this paper are part of a continuing comprehensive experiment, whose completion is planned at the age of 1 year of the samples. Results from electron microscope scanning, mercury porosimetry, and differential thermal analysis are currently being evaluated, and measurements of the resonant frequencies and strength characteristics are continuing. The results will be published in future papers.

Acknowledgements

The experiment and the paper were carried out with the financial support of the Czech Science Foundation under project No. 22-02098S. Partial financial support from the Brno University of Technology via the project FAST-J-23-8287 is also gratefully acknowledged.

References

[1] P. Hrubý, L. Topolář, M. Matysík, I. Plšková. Degradation of materials based on alkali-activated blast-furnace slag after exposure to aggressive environments. *Solid State Phenomena* **325**:131–136, 2021. https://doi.org/10.4028/www.scientific.net/SSP.325.131

[2] C. Shi, P. Krivenko, D. Roy. *Alkali activated cements and concretes*. CRC Press, 2003.

[3] P. Hrubý, V. Bílek, L. Topolář, et al. Resistance of alkali-activated blast furnace slag to acids. *Journal of Physics: Conference Series* **2341**:012002, 2022. https://doi.org/10.1088/1742-6596/2341/1/012002

[4] R. Manjunath, M. C. Narasimhan, K. Umesha. Studies on high performance alkali activated slag concrete mixes subjected to aggressive environments and sustained elevated temperatures. *Construction and Building Materials* **229**:116887, 2019. https://doi.org/10.1016/j.conbuildmat.2019.116887

[5] O. A. Mohamed. A review of durability and strength characteristics of alkali-activated slag concrete. *Materials* **12**(8):1198, 2019. https://doi.org/10.3390/ma12081198

[6] A. Fernández-Jiménez, J. Palomo, F. Puertas. Alkali-activated slag mortars: Mechanical strength behaviour. *Cement and concrete research* **29**(8):1313–1321, 1999. https://doi.org/10.1016/S0008-8846(99)00154-4

[7] V. Bílek Jr, P. Hrubý, V. Iliushchenko, et al. Experimental study of slag changes during the very early stages of its alkaline activation. *Materials* **15**(1):231, 2021. https://doi.org/10.3390/ma15010231

[8] Z. Li, T. Lu, X. Liang, et al. Mechanisms of autogenous shrinkage of alkali-activated slag and fly ash pastes. *Cement and Concrete Research* **135**:106107, 2020. https://doi.org/10.1016/j.cemconres.2020.106107

[9] M. B. Haha, G. Le Saout, F. Winnefeld, B. Lothenbach. Influence of activator type on hydration kinetics, hydrate assemblage and microstructural development of alkali activated blast-furnace slags. *Cement and Concrete Research* **41**(3):301–310, 2011. https://doi.org/10.1016/j.cemconres.2010.11.016

[10] C. D. Atiş, C. Bilim, Ö. Çelik, O. Karahan. Influence of activator on the strength and drying shrinkage of alkali-activated slag mortar. *Construction and building materials* **23**(1):548–555, 2009. https://doi.org/10.1016/j.conbuildmat.2007.10.011

[11] Y. Zuo, G. Ye. Pore structure characterization of sodium hydroxide activated slag using mercury intrusion porosimetry, nitrogen adsorption, and image analysis. *Materials* **11**(6):1035, 2018. https://doi.org/10.3390/ma11061035

[12] ASTM C666/C666M – 15 Standard Test Method for Resistance of Concrete to Rapid Freezing and Thawing, ASTM International, 2015.

[13] CEN/TR 15177 Testing the freeze-thaw resistance of concrete – Internal structural damage (European Committee for Standardization, Brussels, 2006).

[14] D. Kocáb, T. Vymazal, T. Komárková, M. Lišovský. Methods for evaluation of freeze-thaw resistance of concrete and their comparison. *AIP Conference Proceedings* **2780**(1):020032, 2023. https://doi.org/10.1063/5.0136986

[15] V. Bílek Jr, R. Novotný, J. Koplík, et al. Philosophy of rational mixture proportioning of alkali-activated materials validated by the hydration kinetics of alkali-activated slag and its microstructure. *Cement and Concrete Research* **168**:107139, 2023. https://doi.org/10.1016/j.cemconres.2023.107139

[16] ČSN EN 1015–3. Zkušební metody malt pro zdivo – Část 3: Stanovení konzistence čerstvé malty (s použitím střásacího stolku) [Methods of test for mortar for masonry – Part 3: Determination of consistence of fresh mortar (by flow table)], (ČNI, Prague, 2000), Czech version of EN 1015–3.

[17] ČSN EN 1015–6. Zkušební metody malt pro zdivo – Část 6: Stanovení objemové hmotnosti čerstvé malty [Methods of test for mortar for mansory – Part 6: Determination of bulk density of fresh mortar], (ČNI, Prague, 1999), Czech version of EN 1015–6.

[18] ASTM C215–19 Standard Test Method for Fundamental Transverse, Longitudal, and Torsional Resonant Frequencies of Concrete Specimens, ASTM International, 2019.

[19] ČSN EN 196–1. Metody zkoušení cementu. Část 1: Stanovení pevnosti [Methods of testing cement – Part 1: Determination of strength], (ČNI, Prague, 2016), Czech version of EN 196–1.

[20] D. Kocáb, M. Kralikova, P. Cikrle, et al. Experimental analysis of the influence of concrete curing on the development of its elastic modulus over time. *Materials and Technoly* **51**(4):657–665, 2017. https://doi.org/10.17222/mit.2016.248

[21] A. Neville. *Properties of Concrete*. Pearson, 2011.

[22] D. Chen, J. Zou, L. Zhao, et al. Degradation of dynamic elastic modulus of concrete under periodic temperature-humidity action. *Materials* **13**(3):611, 2020. https://doi.org/10.3390/ma13030611

[23] V. Afroughsabet, L. Biolzi, P. J. Monteiro. The effect of steel and polypropylene fibers on the chloride diffusivity and drying shrinkage of high-strength concrete. *Composites Part B: Engineering* **139**:84–96, 2018. https://doi.org/10.1016/j.compositesb.2017.11.047

[24] M. Safiuddin, S. N. Raman, M. F. M. Zain. Non-destructive evaluation of flowing concretes incorporating quarry waste. *Australian Journal of Basic and Applied Sciences* **1**(2):87–95, 2007.

[25] C. Gheorghiu, J. E. Rhazi, P. Labossière. Impact resonance method for fatigue damage detection in reinforced concrete beams with carbon fibre reinforced polymer. *Canadian Journal of Civil Engineering* **32**(6):1093–1102, 2005. https://doi.org/10.1139/l05-064

[26] Y. Akkaya, C. Ouyang, S. P. Shah. Effect of supplementary cementitious materials on shrinkage and crack development in concrete. *Cement and Concrete Composites* **29**(2):117–123, 2007. https://doi.org/10.1016/j.cemconcomp.2006.10.003